Nano Energy (2015) 11, 756–764

Available online at www.sciencedirect.com

ScienceDirect

journal homepage: www.elsevier.com/locate/nanoenergy

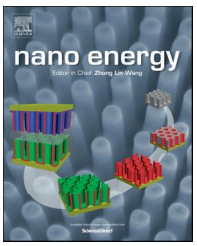

RAPID COMMUNICATION

Broadband light-concentration with near-surface distribution by silver capped silicon nanowire for high-performance solar cells

Yingfeng Li[a], Meicheng Li[a,b,*], Dandan Song[a], Hong Liu[c], Bing Jiang[a], Fan Bai[d], Lihua Chu[a]

[a]*State Key Laboratory of Alternate Electrical Power System with Renewable Energy Sources, North China Electric Power University, Beijing, 102206, China*
[b]*Su Zhou Institute, North China Electric Power University, Suzhou, 215123, China*
[c]*State Key Laboratory of Crystal Materials, Shandong University, Jinan 250100, China*
[d]*Yunnan Institute of Products Quality Inspection, Yunnan, 650000, China*

Received 2 November 2014; accepted 26 November 2014
Available online 4 December 2014

KEYWORDS
Silver cap;
Silicon nanowire;
Broadband;
Near-surface distribution

Abstract
Silicon nanowire (SiNW) shows striking light-concentration ability and thus holds promising application potentials in photonic devices. However, its narrow working waveband strongly affects its performance over the entire visible spectrum. Here, a silver capped SiNW structure (Ag-cap/SiNW) is presented to broaden the working waveband of the pure SiNW. Discrete dipole approximation simulations show that, by this structure, the light-concentration waveband can be significantly broadened from 440–620 nm (pure SiNW) to 300–620 nm. Thus, using the Ag-cap/SiNW in the solar cell, the ideal photocurrent density can be enhanced 16% compared with that using pure SiNW. Furthermore, the concentrated light shows the feature of the strong near-surface distribution around the Ag-cap/SiNW. This distribution feature gives a reasonable explanation for the huge superiority of the radial junction SiNW solar cells to axial junction SiNW solar cells from optical aspect. Additionally, due to the intrinsic waveguide property of SiNW, this Ag-cap/SiNW also has great potential applications in photonic devices such as nanoscale optical biosensors and light-integrated-chips.

*Corresponding author at: State Key Laboratory of Alternate Electrical Power System with Renewable Energy Sources, North China Electric Power University, Beijing, 102206, China.
E-mail address: mcli@ncepu.edu.cn (M. Li).

http://dx.doi.org/10.1016/j.nanoen.2014.11.054
2211-2855/

Introduction

Silicon nanowire (SiNW) is attracting an increasing interest in recent years [1-6]. Among other excellent properties, its unique optical properties, the ability to capture and concentrate light with regional transverse distribution at nanoscale [7-11] makes it hold promise for potential applications as nanoscale building blocks in photonic devices: SiNW based solar cells [12-15], sunlight-driven solar water splitting [16], nanoelectronic power sources [17,18], photoelectrochemical cell [1,19], photodetectors [20,21], and even the fascinating light-integrated-chip [22].

The main drawback of using SiNW as light concentrator is that it only works at various narrow wavebands [11,23,24], which correspond to the resonance wavelengths of the lowest-order leaky mode supported by the SiNW [25,26]. These narrow working wavebands strongly limit its performance over the entire visible spectrum, and thus limit its practical application in some fields. For instance, in photovoltaic cells [13-15,17,27] and photoelectrochemical cells [1], broadband light-concentration is of great concern to ensure maximum utilization of the sunlight to generate high photocurrent. In sunlight-driven solar water splitting [16], a broader light-concentration waveband is also very helpful to achieve higher splitting efficiency by generating more photogenerated carries.

Fortunately, silver nanoparticle also possesses outstanding light-concentration function [28-30] due to the plasmonic effect, and at the same time its working waveband is rightly complementary with that of the SiNW. So, combining the silver nanoparticle and the SiNW together as a composite structure should be one possible way to avoid the limitation of the SiNW in broadband light-concentration.

To date, only few works on silver-nanoparticle/SiNW composite structure has been reported [23,31,32], and the broadband light-concentration ability hasn't been realized in all of them. For instance, in Ref. [31] where a silver nanoparticles decorated SiNW structure was presented, only the light-concentration ability of the silver nanoparticles (about 50-fold) was highlighted but that of the SiNW was almost vanished. We think that the failure of the silver nanoparticles decorated SiNW in broadband light- concentration is mainly due to the high density of the silver nanoparticles, which wholly shield the light-concentration function of the SiNW by abundant geometrical scatterings.

So, in this work, a silver nanoparticle capped SiNW structure (Ag-cap/SiNW) is designed to realize the broadband light-concentration function. The single silver cap (Ag-cap) can only cover a small geometrical area, thus will not affect the light-concentration ability of the SiNW significantly. Besides, in this Ag-cap/SiNW structure, the concentrated light could be further expected to distribute regionally in transverse direction as that in the pure SiNW [7-11]. This is because the light concentrated by the Ag-cap has great tendency to be unidirectionally scattered into the SiNW, thus to be coupled into the guided modes following their field distribution. This regional transverse distribution is of great importance in photonic devices optimization [7]. In a word, by the Ag-cap/SiNW, a broadband light-concentration function with regional transverse distribution is expected to be realized.

Based on discrete dipole approximation (DDA) method [33-35], the optical properties of the Ag-cap/SiNW are investigated in detail. The two expected light-concentration functions are both realized. The light-concentration waveband is broadened from 440-620 nm (pure SiNW) to 300-620 nm, which brings a 16% enhancement of ideal photocurrent density in solar cell using the Ag-cap/SiNW compared with that using the pure SiNW. The concentrated light distributes regionally in transverse direction, and thus shows a feature of the strong near-surface distribution within and out the silicon part. This provides reasonable optical explanation for the superiority of radial junction to axial junction SiNW solar cells. Such insight is essential to the design and optimization of the efficient solar cells and other optical devices.

Model, simulation method and reliability testing

A schematic diagram of the presented Ag-cap/SiNW is shown in Fig. 1a. The Ag-cap is designed with hemispherical end for easily preparing [36]. The size parameters are set referring to the reported well performed SiNW solar cells. The diameter is set to 80 nm, which corresponds to the optimized light-trapping effect [37]. The total length is set to 3.0 μm, which approximates to the average of the values, 1.5 to 4 μm [37,38], for optimized conversion efficiency. To make the light-concentration effect of the Ag-cap remarkable (see the Supporting Information), its length is set as 0.7 μm. Since the diameter is large enough, the quantum confinement effect [13,39] is neglected and thus the complex dielectric constants of bulk silver and silicon, as shown in Fig. 1b and c, are used [40,41]. Besides, only the incident light from the Ag-cap is considered as the light-trapping effect of SiNW is insensitive to the incident angle [24].

The extinction, scattering and absorption spectra of the Ag-cap/SiNW, as well as the light filed distribution within it are calculated using the DDA method by code DDSCAT 7.3 [33]. Firstly, the Ag-cap/SiNW is replaced by an array of point dipoles, located on cubic lattices. Then, the electromagnetic scattering problem of the incident light interacting with this point dipoles array is solved. Finally, the spectrum and light field distribution properties are derived. A frame description of the DDA method is given as follows.

Let the index $j=1,\ldots N$ run over the occupied lattice sites. Each dipole j is characterized by a polarizability tensor α_j, Such that $\vec{P}_j=\alpha_j\vec{E}_{\mathrm{ext},j}$, where $\vec{P}_j$ is the instantaneous dipole moment of dipole j, and $\vec{E}_{\mathrm{ext},j}$ is the instantaneous electric field at position j due to the incident light on the dipole plus the other $N-1$ oscillating dipoles. The key problem in DDA is to obtain a self-consistent set of dipole moments $\vec{P}_j$. $\vec{P}_j=\alpha_j\vec{E}_{\mathrm{ext},j}$ can be rewritten as N simultaneous complex vector equation of the form

$$\vec{P}_j=\alpha_j(\vec{E}_{\mathrm{inc},j}-\sum_{k\neq j}A_{jk}\vec{P}_k) \tag{1}$$

where $\vec{E}_{\mathrm{inc},j}$ is the electric field at position j due to the incident light, and $-A_{jk}\vec{P}_k$ is the contribution to the electric field at position j due to the dipole at position k.

$$\vec{E}_{\mathrm{inc},j}=\vec{E}_0\exp(i\vec{k}\cdot\vec{r}_j-i\omega t)$$

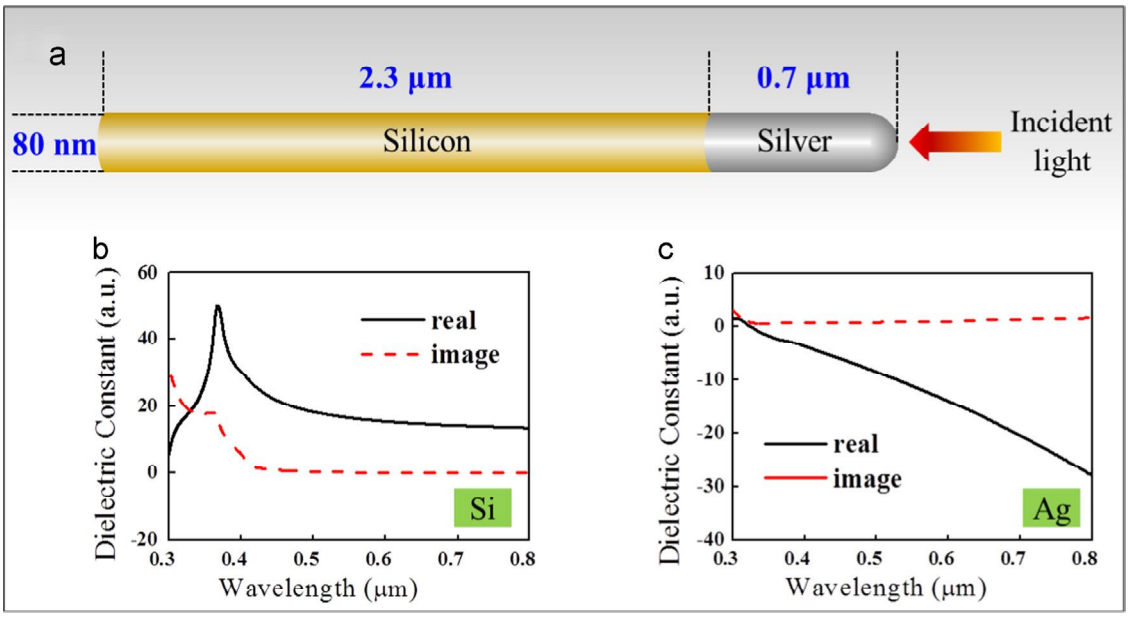

Fig. 1 Schematic diagram of the model and dielectric constants of silicon and silver. (a) the model of the Ag-cap/SiNW; (b) the dielectric constant of the silicon; (c) the dielectric constant of the silver.

$$\vec{P}_k\vec{P}_j = \frac{\exp(ikr_{jk})}{r_{jk}^3}\left\{k^2\vec{r}_{jk}\times(\vec{r}_{jk}\times\vec{P}_k)+\frac{(1-ikr_{jk})}{r_{jk}^2}\times\left[\qquad\qquad\right]\right\}\quad(j\neq k) \tag{3}$$

where $\vec{r}_{jk}\equiv\vec{r}_j-\vec{r}_k$. If A_{jj} is defined as $A_{jj}=\alpha_j^{-1}$, the scattering problem can be compactly formulated as a set of N inhomogeneous linear complex vector equations:

$$\sum_{k=1}^{N}A_{jk}\vec{P}=\vec{E}_{\mathrm{inc},j}\quad(j=1,\ldots,N) \tag{4}$$

It is further convenient to define $3N$-dimensional vectors $\tilde{P}=(\vec{P}_1,\vec{P}_2,\ldots\vec{P}_N)$, $\tilde{E}_{\mathrm{inc}}=(\vec{E}_{\mathrm{inc},1},\vec{E}_{\mathrm{inc},2},\ldots\vec{E}_{\mathrm{inc},N})$, and a $3N\times3N$ matrix $\tilde{A}$ so that the problem is reduced to a single matrix equation:

$$\tilde{A}\tilde{P}=\tilde{E} \tag{5}$$

Direct methods for solving this system of equations for the unknown $\tilde{P}$ are impractical, but iterative methods are useful. An error tolerance between two adjacent iterative steps is specified as

$$h=\frac{|\tilde{A}^{\dagger}\tilde{A}\tilde{P}-\tilde{A}^{\dagger}\tilde{E}|}{|\tilde{A}^{\dagger}\tilde{E}|} \tag{6}$$

where $\tilde{A}^{\dagger}$ is the hermitian conjugate of $\tilde{A}$. In our calculations, the recommended PBCGS2 iteration algorithm is chosen, and an error tolerance $h=1.0\times10^{-5}$, corresponding to high accuracy [33] is used.

After the polarizations $\vec{P}_j$ are obtained, the extinction, absorption and scattering cross section for the target are then computed as:

$$C_{\mathrm{ext}}=\frac{4\pi k}{|\vec{E}_{\mathrm{inc}}|^2}\sum_{j=1}^{N}\mathrm{Im}(\vec{E}_{\mathrm{inc},j}^{*}\times\vec{P}_j) \tag{7}$$

$$C_{\mathrm{abs}}=\frac{4\pi k}{|\vec{E}_{\mathrm{inc}}|^2}\sum_{j=1}^{N}\left\{\qquad\qquad\right\} \tag{8}$$

$$C_{\mathrm{sca}}=C_{\mathrm{ext}}-C_{\mathrm{abs}} \tag{9}$$

and the corresponding extinction, absorption and scattering efficiency factors for the target are written as:

$$Q_{\mathrm{ext}}=\frac{C_{\mathrm{ext}}}{\pi r^2} \tag{10}$$

$$Q_{\mathrm{abs}}=\frac{C_{\mathrm{abs}}}{\pi r^2} \tag{11}$$

$$Q_{\mathrm{sca}}=\frac{C_{\mathrm{sca}}}{\pi r^2} \tag{12}$$

where r is the real geometric radius of Ag-cap/SiNW in this work.

The reliability of the DDA method on silver and silicon nanostructures has been evaluated by comparing the calculation results with that derived from rigorous electromagnetic theory [42,43] and that of our experimental measurements, respectively (see the Supporting Information). Excellent consistency is obtained between the DDA results and the theoretical and the experimental results. The accuracy of the DDA method is mainly depending on the interdipole separation d. By comparing the calculated extinction spectra of the Ag-cap/SiNW under the d values ranging from 2.8 nm to 9.6 nm, it is ens d=3.3 nm, which is chosen in following calcul accurate enough (see the Supporting Information

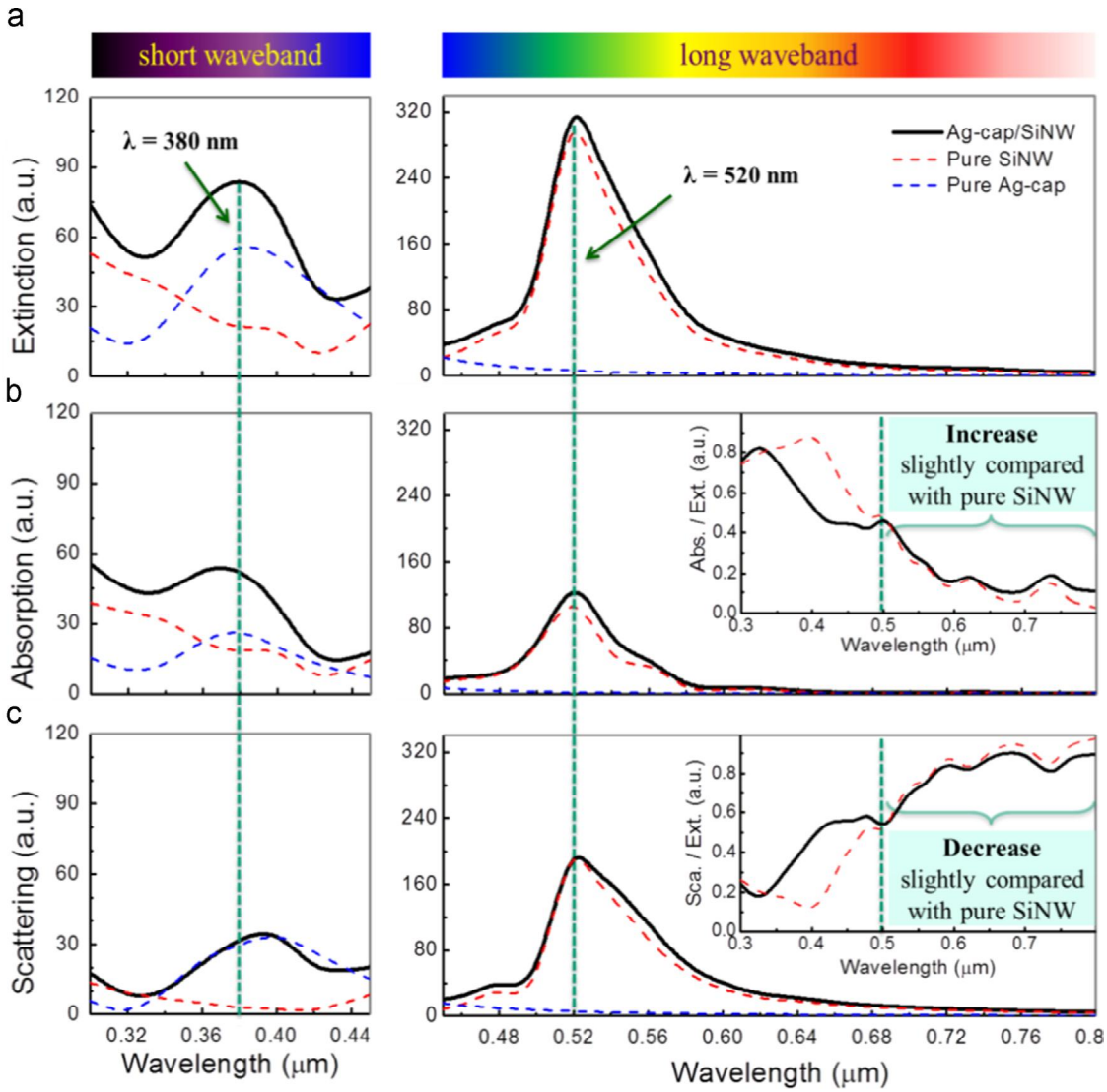

Fig. 2 The extinction, absorption and scattering efficiency spectra, for the Ag-cap/SiNW and the separated pure SiNW and Ag-cap: (a) the extinction spectra, (b) the absorption spectra, (c) the scattering spectra. The rations between the absorption, scattering efficiency and the extinction efficiency are given in the insets of (b) and (c), respectively.

Results and discussion

Broad spectrum light-concentration ability of the Ag-cap/SiNW

What's shown in Fig. 2 is the extinction, absorption and scattering efficiency spectrum curves of the Ag-cap/SiNW. And for results analysis, the curves for the separated pure SiNW and Ag-cap are also given. Additionally, the absorption and the scattering fractions in the concentrated light, characterized by Q_{abs}/Q_{ext} and Q_{sca}/Q_{ext}, are provided yet in the insets of Fig. 2b and c, respectively.

From Fig. 2a, the extinction curves, it can be observed obviously that the Ag-cap/SiNW shows two prominent extinction peaks, whose values are much greater than 1, at wavelength λ=380 nm and 520 nm. Since the value of Q_{ext} represents the light-concentration multiple of the target according to above definition, these two peaks imply that the Ag-cap/SiNW will own outstanding light-concentration ability in two wavebands with centric wavelength 380 nm and 520 nm. The waveband around 520 nm can be conceivably attributed to the contribution of the silicon part, as the extinction curves in this waveband are exactly anastomotic with that of the pure SiNW. The 380 nm waveband should be mainly assigned to the contribution of the Ag-cap since the extinction curves shows the similar variation as that of the pure Ag-cap.

It can be also observed in Fig. 2a that the extinction curve of the pure SiNW only owns one peak at λ=520 nm, which implies only one light-concentration waveband. So, the Ag-cap/SiNW will own broader light-concentration waveband than pure SiNW. If taking the concentration multiple 35 as a criterion, the working waveband of the Ag-cap/SiNW can be broadened from 440-620 nm (pure SiNW) to 300-620 nm, which just corresponds to the high energy density waveband in the solar spectrum. To quantitatively evaluate the effect brought by this bro we define and calculate an enhancement factor R_e waveband 300-800 nm as below:

$$R_e = \frac{\int_{300\ nm}^{800\ nm} Q_{ext(Ag-cap/SiNW)} d\lambda - \int_{300\ nm}^{800\ nm} Q_{ext(pure-Si)} d\lambda}{\int_{300\ nm}^{800\ nm} Q_{ext(pure-Si)} d\lambda} \quad (13)$$

where $Q_{ext(Ag\text{-}cap/SiNW)}$ and $Q_{ext(pure\text{-}Si)}$ are the extinction efficiency of the Ag-cap/SiNW and the pure SiNW, respectively. A value R_e=34% is obtained.

The superior light-concentration ability of the Ag-cap/SiNW over pure SiNW should mainly come from the contribution of the Ag-cap, which works in 320-440 nm as shown in Fig. 2a. This can be confirmed experimentally by the fact that SiNW arrays will show high reflectance in 320-440 nm [44] under sunlight irradiation. Besides, the superiority light-concentration ability of the Ag-cap/SiNW may also have contributions from the mutual enhancement effects of the silver and silicon parts in light-concentration. As shown in Fig. 2a, the extinction curve of the Ag-cap/SiNW is significantly larger than that of the pure Ag-cap in the short waveband, and is slightly larger than that of the pure SiNW in the long waveband, respectively.

Taking into account the considerable ohmic loss in metal nanoparticle around its resonance wavelength [45,46], it is necessary to ensure that the concentrated light is not completely lost thus is significative for photovoltaic applications. Fig. 3 gives the square of the electric field intensity (equals to the light intensity) within the Ag-cap/SiNW and pure SiNW, under irradiation of light with λ=380 nm. The light intensity in the silicon part of the Ag-cap/SiNW is two-fold of that in the pure SiNW (25-.vs. 12.5-fold of the incident light intensity), which indicates amount of the light concentrated by the Ag-cap has been scattered into the silicon. This provides a direct argument for the significant of the light concentrated by the Ag-cap.

The proportion of light being absorbed by the Ag-cap (ohmic loss) at λ=380 nm can be estimated quantitatively based on the light absorption formula $P_{abs}=I_{light}\bullet c\bullet\alpha$, which indicates the amount of light being absorbed P_{abs} is proportional to light intensity I_{light}. In the following, P_{abs} is represented by the absorption efficiency (Q) defined above. Firstly, the amount of light being absorbed in the silicon part of the Ag-cap/SiNW ($Q_{abs,si}$) is calculated by doubling that in the pure SiNW ($Q_{abs,pure\_si}$=18.5, Fig. 2b), that is, $Q_{abs,si}$=37.0. Secondly, the amount of light being absorbed in the Ag-cap ($Q_{abs,Ag}$) is calculated by subtracting $Q_{abs,si}$ from that in the Ag-cap/SiNW ($Q_{abs,Ag\text{-}Si}$=52.0, Fig. 2b), that is, $Q_{abs,Ag}$=15.0. Finally, the proportion of ohmic loss in the whole amount of light being concentrated can be estimated as $Q_{abs,Ag}/Q_{ext,Ag\text{-}Si}$=18.0%, where $Q_{ext,Ag\text{-}Si}$ (83.5, Fig. 2a) is the extinction efficiency of the Ag-cap/SiNW.

Except for the part being lost, the left light concentrated will have two outcomes: being scattered out or being absorbed by the silicon. From the inset in Fig. 2c it can be observed that the scattered light occupies a large ratio, which reach 38.0% and 48.0% for λ=380 nm and 520 nm, respectively. Thus, to investigate the scattering features of these light is of great importance for the fully utilization of them. In Fig. 4, the angle distributions in resolution 5° for the scattered light with λ=380 nm and 520 nm are plotted, respectively. And their forward scattering fractions (FSF) are obtained by calculating the ratio between the integral of scattering intensity in range 0°-90° and that in range 0°-180°. As illustrated, the FSF of the light with λ=380 nm and 520 nm reaches 98.9% and 99.7%, respectively. These high FSFs mean that the most of the scattered light is still possible to be captured, for example, by a substrate, and has great potential to be well utilized in the design of the novel devices.

Additionally, for the light with λ=380 nm, the FSF of the Ag-cap/SiNW is 3.4% and 4.3% greater than that of the pure SiNW (Fig. 4b) and the pure Ag-cap (94.6%, not plotted), respectively. This indicates the Ag-cap and the SiNW can enhance the forward scattering each other. From the insets in Fig. 2b it can be seen that the absorbed fractions in the Ag-cap/SiNW are greater than those in pure SiNW when λ>500 nm. This indicates the Ag-cap has the capacity to enhance the light absorption within the silicon part in long waveband. The enhanced forward scattering and absorption

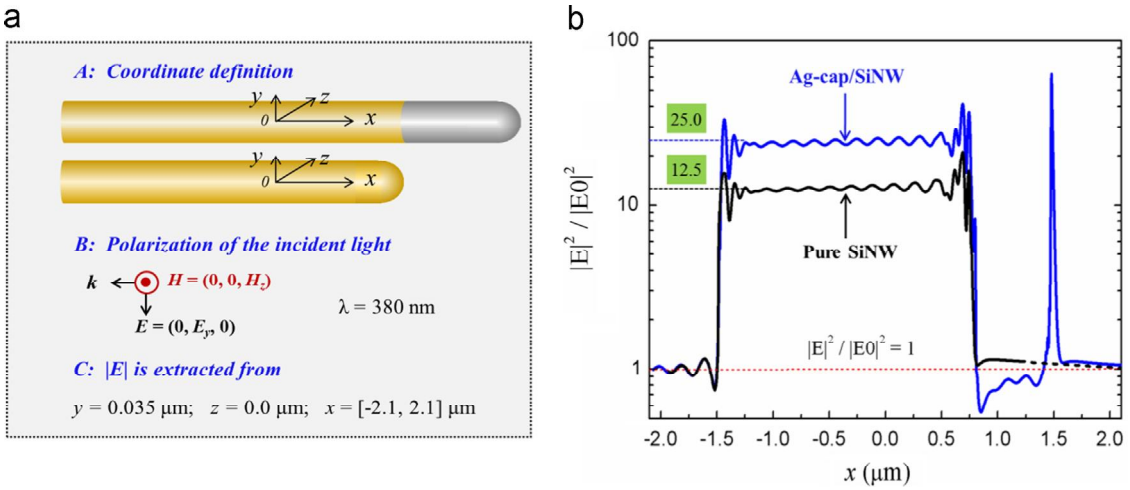

Fig. 3 The axial variation of $|E|^2/|E_0|^2$ along the Ag-cap/SiNW and the pure SiNW, for light with wavelength 380 nm. (a) ex for the data sources: the definition of coordinates, the incident light polarization and the positions where |E| is extra (b) the variation curves of $|E|^2/|E_0|^2$. The positions y=0.035 μm, z=0.0 μm correspond to the most intensive electric f silicon part of the Ag-cap/SiNW and the pure SiNW.

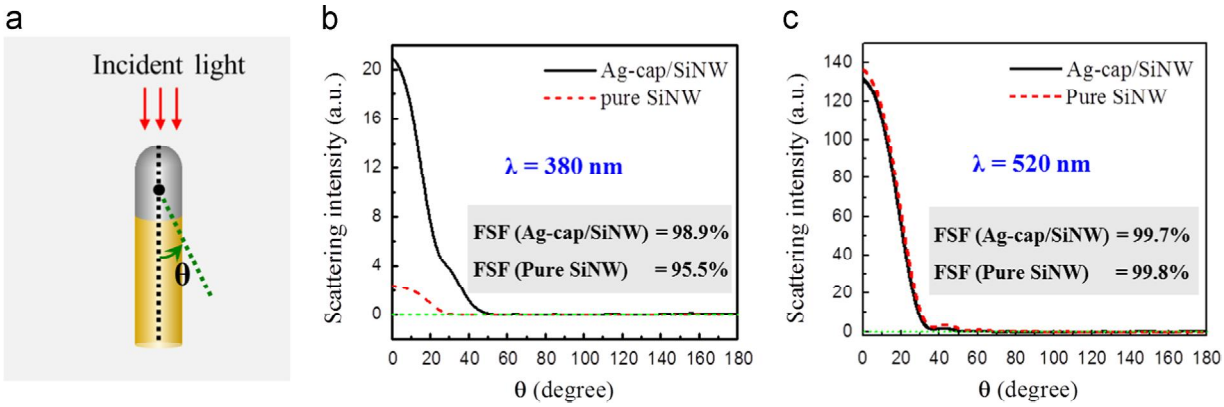

Fig. 4 The angle distribution of scattering intensity around the Ag-cap/SiNW and pure SiNW in angular resolution 5° for light with wavelength 380 and 520 nm. (a) the definition of θ; (b) the distribution for light with λ=380 nm; (c) the distribution for light with λ=520 nm.

mean more tight confinement on the concentrated light, and thus are of positive significance in future applications. Moreover, these two phenomena are similar to those occurred on the structure with silver particles deposited on bulk substrate [45,47], and thus can be also explained by the function of metal particles in redirecting light preferentially into the high-index substrate [44].

The light distribution within and out the Ag-cap/SiNW

From above discussions, it has been demonstrated that the Ag-cap/SiNW owns excellent light-concentration ability in broadband. While, to shed the concentrated light upon the critical issues in the future photovoltaic or other photonic applications of this Ag-cap/SiNW, it is also of great importance to accurately make clear the light distribution features within and out it.

We pay attentions to the distribution of light out the Ag-cap/SiNW (scattering light) firstly. Based on the angle distribution curves in Fig. 4, it can be observed that most of the scattering light tends to distribute in a narrow angle range, θ<20°, around the Ag-cap/SiNW. Over 79% and 87% of the scattering light with λ=380 nm and 520 nm will be confined in a conical space with cone angle of 20°, respectively.

Then, we focus on the distribution of light within the Ag-cap/SiNW (absorption light). Fig. 5 gives the distribution of the electric field, whose square is equal to the light intensity, in the Ag-cap/SiNW. To deliver a better view of the light intensity variation in the lateral direction, the *x*-axis and *y*-axis aspect ratio has been intentionally enlarged to 3:1. It can be seen from Fig. 5a. In1 and Fig. 5b. In1 that, for both the light with λ=380 nm and 520 nm, the field is not uniform throughout the cross section but tends to localize near the surface of the SiNW. To describe these near-surface distribution features more clearly, we divide the cross section into 100 annuluses with identical Δr, integrate the square of the field intensities over every annulus, and give the radial distribution of these integrations in Fig. 5a. In2 and Fig. 5b. In2. Over 95% and 91% of the absorption light with λ=380 nm and 520 nm will localize in a near-surface layer of the SiNW with 20 nm thickness, respectively.

As a summary, the concentrated light by the Ag-cap/SiNW, no matter within or out it, no matter with short or long wavelength, both shows the strong near-surface distribution feature.

Application prospects of the Ag-cap/SiNW

In above, the light-concentration features of the Ag-cap/SiNW have been studied in detail based on DDA method. According to the previous research [48] and our verification calculations (see the Supporting Information), the DDA method can give reliable results. Therefore, the following application prospects based on the calculation results will be reliable still.

The significantly broadened light-concentration waveband 300–620 nm of the Ag-cap/SiNW comparing with that of pure SiNW, 440–620 nm, indicates that this structure has stronger sunlight harvesting ability than pure SiNW and thus has great potential in high-performance solar cells applications.

Firstly, the number of solar photons trapped effectively per unit time and sectional area by a single Ag-cap/SiNW is estimated under an *AM1.5* spectrum over 300–800 nm. This can be represented and calculated by the solar-spectrum weighted effective light-harvesting efficiency, $Q_{\text{ssw-elt}}$

$$Q_{\text{ssw-elt}} \equiv \int_{300}^{800} W_{\text{AM1.5}}(\lambda)[Q_{\text{ext}}(\lambda) - Q_{\text{sca-}b}(\lambda) - Q_{\text{ohm-loss}}(\lambda)]d\lambda \tag{14}$$

where $W_{\text{AM1.5}}(\lambda)$ is the weighting factor derived from $\int_{300}^{800} W_{\text{AM1.5}}(\lambda)d\lambda = 1$, $Q_{\text{ext}}(\lambda)$ is the extinction efficiency, $Q_{\text{sca-b}}(\lambda)$ is the back scattering efficiency (taken as $1\% \times Q_{\text{sca}}$ over 300–800 nm according to Fig. 4). $Q_{\text{ohm-loss}}(\lambda)$ is the ohmic losses efficiency (taken as $18\% \times Q_{\text{ext}}(\lambda)$ over 320–440 nm and 0 in other waveband). The obtained $Q_{\text{ssw-elt}}$ is 72.0, which is 28% larger than that of the pure SiNW, 56.2.

Secondly, an enhancement of the short-circuit photocurrent density J_{sc} in solar cell using this Ag-cap/SiNW o
using pure SiNW is estimated theoretically. Ur
assumption that the forward scattered light can
completely utilized, the J_{sc} of a solar cell can be ca

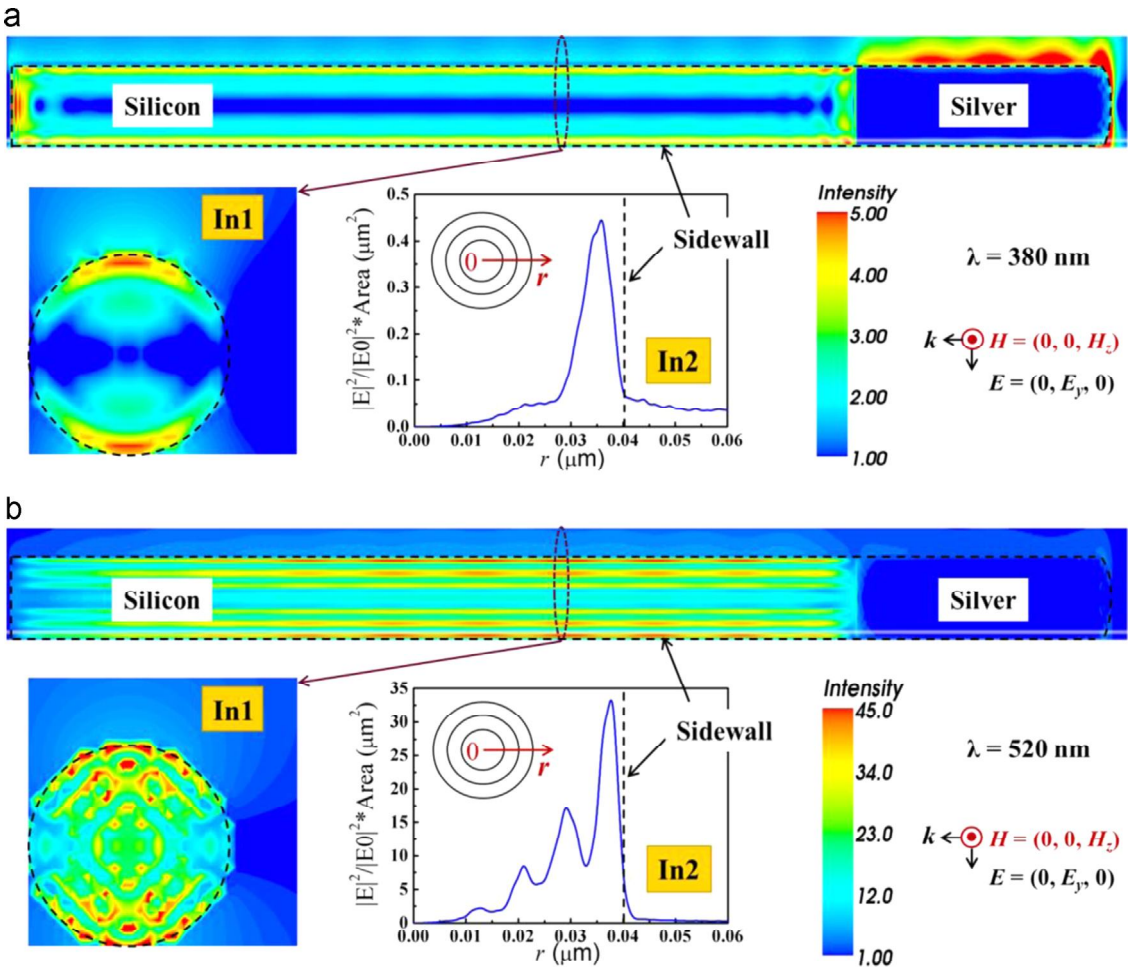

Fig. 5 The electric field distributions in the Ag-cap/SiNW. (a) for light with λ=380 nm; (b) for light with λ=520 nm. In each subgraph: the vertical section; one cross section, labeled In1; and the radial distribution of the integrated square of the field intensity ($|E_0|^2/|E|^2$*area) in the cross section, labeled In2, are given. $|E|^2/|E_0|^2$*area is calculated by dividing the cross section into 100 annuluses and integrating $|E|^2/|E_0|^2$ over each of them. The filed intensity is represented by rainbow colors, and the directions of the wave vector, electric and magnetic field for the incident light are illustrated.

as

$$J_{SC} \equiv q \int F_{AM1.5}(\lambda) \times Q_{elt-array}(\lambda) \times IQE d\lambda \tag{15}$$

where, q is the charge carried by one electron; $F_{AM1.5}(\lambda)$ is the spectral photon flux density delivered by the sun [49]; IQE is the internal quantum efficiency, whose value is taken as 100%, according to the recent demonstration [19] on nanowire junction devices; $Q_{elt\text{-}array}(\lambda)$ is the effective light-harvesting efficiency, which equals

$$Q_{elt-array}(\lambda) = \begin{cases} [Q_{ext}(\lambda) - Q_{sca-b}(\lambda) - Q_{ohm-loss}(\lambda)]/Q_{ext}(\lambda) & Q_{ext}(\lambda) \times R \geq 1 \\ [Q_{ext}(\lambda) - Q_{sca-b}(\lambda) - Q_{ohm-loss}(\lambda)] \times R & Q_{ext}(\lambda) \times R < 1 \end{cases} \tag{16}$$

where, R is the cover fraction of nanowire on the substrate, whose value is chosen according to the value of $Q_{ext}(\lambda)$.

Since the values of $Q_{ext}(\lambda)$ are so large (on the order of magnitude 10 to 10^2) in the working waveband of the Ag-cap/SiNW, only a small R is enough to harvest most of the sunlight. In our estimations, R=3.0% is used to almost harvest the sunlight completely but not quite. This is very approximate to the R value used in *Ref.* [37]. As a consequence, the ideal short-circuit photocurrent density of solar cell using the Ag-cap/SiNW is 27.7 mA/cm^2, which shows 16% larger than that using pure SiNW, 23.9 mA/cm^2.

The near-surface distribution feature of the concentrated light within and out the Ag-cap/SiNW is also of great helpful for its application in high-performance solar cells. This distribution feature provides a reasonable optical explanation for the huge superiority of radial junction over axial junction SiNW solar cells (the reported highest conversion efficiency of them is 15.14% [50] and 1.9% [51], respectively): in radial p-n junction SiNW solar cells, the p-n junction fabricated near the nanowire surface is coincidently locate at the strong light zones [7] according to our calculations, thus is very suitable for the generation and timely collection of the photo-carries.

Except for photovoltaic application, the Ag-cap/SiNW also has other potential applications. Since the hen
shape naturally accepts large angles of incidence
structure may have a function to capture and cc
light from various incident angles. At the same time

waveguide ability of SiNW will make the concentrated light being redirected and exported in a unidirectional direction with low loss. So, this Ag-cap/SiNW structure (actually, not limited to silicon but other semiconductor nanowire might as well) could be recognized to be a plasmonic signal-amplifier connected by a unidirectional information highway. Ag-cap/SiNW thus has great application potential in nanoscale plasmonic optical biosensor [53], nano-waveguide [54], or nano-lenses used in future light-integrated-chip [55].

Conclusions

In summary, we present a light-harvesting structure, Ag-cap/SiNW, and report comprehensive investigations on its optical properties by the DDA method. This Ag-cap/SiNW presents two outstanding optical features. The first one is that it shows a broadband light-concentration ability in waveband 300–620 nm, which results in that it owns significant superiority over pure SiNW in light-harvesting: a 28% enhanced effective light-harvesting efficiency is obtained. This light-harvesting ability makes the ideal photocurrent density in solar cell using Ag-cap/SiNW show 16% higher than that using pure SiNW. The second feature is that the light concentrated by the Ag-cap/SiNW shows strong near-surface distribution feature within and out the silicon nanowire, which gives a reasonable explanation for the huge superiority of radial junction SiNW solar cells over axial junction SiNW solar cells from the optical aspect. Except for photovoltaic applications, this Ag-cap/SiNW structure also shows potential applications in nanoscale optical devices such as optical biosensors or light-integrated-chips. The findings obtained herein can provide insightful guidelines for structural design, optimization, and thus improve performance for future solar cell and other optical devices.

Acknowledgments

IThis work is partially supported by National Natural Science Foundation of China (Grant nos. 51402106, 51372082, 51172069, 50972032, 61204064, 51202067 and 91333122), Ph.D. Programs Foundation of Ministry of Education of China (Grant nos. 20110036110006, 20120036120006, 20130036110012), Science and Technology Program Foundation of Suzhou City (SYG201215), and the Fundamental Research Funds for the Central Universities.

Appendix A. Supporting information

Supplementary data associated with this article can be found in the online version at http://dx.doi.org/10.1016/j.nanoen.2014.11.054.

References

[1] R.H. Coridan, K.A. Arpin, B.S. Brunschwig, P.V. Braun, N.S. Lewis, Nano Lett. 14 (2014) 2310–2317.
[2] K.-Q. Peng, X. Wang, L. Li, Y. Hu, S.-T. Lee, Nano Today 8 (2013) 75–97.
[3] T.J. Kempa, R.W. Day, S.-K. Kim, H.-G. Park, C.M. Lieber, Energ. Environ. Sci 6 (2013) 719–733.
[4] F. Patolsky, G. Zheng, C.M. Lieber, Nat. Protoc. 1 (2006) 1711–1724.
[5] Y. Cui, C.M. Lieber, Science 291 (2001) 851–853.
[6] F. Bai, M. Li, D. Song, H. Yu, B. Jiang, Y. Li, Appl. Surf. Sci. 273 (2013) 107–110.
[7] L. Yu, S. Misra, J. Wang, S. Qian, M. Foldyna, J. Xu, Y. Shi, E. Johnson, P.R. I Cabarrocas, Sci. Rep. 4 (2014) 1–7.
[8] Y. Zhan, X. Li, Y. Li, IEEE J. Sel. Top. Quant. 19 (2013) 1–8.
[9] T. Coenen, J. van de Groep, A. Polman, ACS Nano 7 (2013) 1689–1698.
[10] S.-K. Kim, R.W. Day, J.F. Cahoon, T.J. Kempa, K.-D. Song, H.-G. Park, C.M. Lieber, Nano Lett. 12 (2012) 4971–4976.
[11] L. Cao, J.S. White, J.-S. Park, J.A. Schuller, B.M. Clemens, M.L. Brongersma, Nat. Mater. 8 (2009) 643–647.
[12] R. Yu, Q. Lin, S.-F. Leung, Z. Fan, Nano Energ. 1 (2012) 57–72.
[13] J.K. Mann, R. Kurstjens, G. Pourtois, M. Gilbert, F. Dross, J. Poortmans, Prog. Mater. Sci. 58 (2013) 1361–1387.
[14] T. Song, S.-T. Lee, B. Sun, Nano Energ. 1 (2012) 654–673.
[15] F. Bai, M. Li, R. Huang, Y. Li, M. Trevor, K.P. Musselman, RSC Adv. 4 (2014) 1794–1798.
[16] X. Wang, K.-Q. Peng, Y. Hu, F.-Q. Zhang, B. Hu, L. Li, M. Wang, X.-M. Meng, S.-T. Lee, Nano Lett. 14 (2013) 18–23.
[17] B. Tian, X. Zheng, T.J. Kempa, Y. Fang, N. Yu, G. Yu, J. Huang, C.M. Lieber, Nature 449 (2007) 885–889.
[18] D. Dávila, A. Tarancón, C. Calaza, M. Salleras, M. Fernández-Regúlez, A. San Paulo, L. Fonseca, Nano Energ. 1 (2012) 812–819.
[19] A.P. Goodey, S.M. Eichfeld, K.K. Lew, J.M. Redwing, T.E. Mallouk, J. Am. Chem. Soc. 129 (2007) 12344–12345.
[20] J. Svensson, N. Anttu, N. Vainorius, B.M. Borg, L.-E. Wernersson, Nano Lett. 13 (2013) 1380–1385.
[21] L.Y. Cao, J.S. Park, P.Y. Fan, B. Clemens, M.L. Brongersma, Nano Lett. 10 (2010) 1229–1233.
[22] A. Melloni, A. Canciamilla, C. Ferrari, F. Morichetti, L. O'Faolain, T. Krauss, R. De La Rue, A. Samarelli, M. Sorel, IEEE Photonic J 2 (2010) 181–194.
[23] S. Brittman, H. Gao, E.C. Garnett, P. Yang, Nano Lett. 11 (2011) 5189–5195.
[24] L. Cao, P. Fan, A.P. Vasudev, J.S. White, Z. Yu, W. Cai, J.A. Schuller, S. Fan, M.L. Brongersma, Nano Lett. 10 (2010) 439–445.
[25] K.T. Fountaine, C.G. Kendall, H.A. Atwater, Opt. Express 22 (2014) 930–940.
[26] R. Paniagua-Domínguez, G. Grzela, J.G. Rivas, J. Sánchez-Gil, Nanoscale 5 (2013) 10582–10590.
[27] F. Bai, M. Li, R. Huang, D. Song, B. Jiang, Y. Li, Nanoscale Res. Lett. 7 (2012) 557–561.
[28] J.A. Schuller, E.S. Barnard, W. Cai, Y.C. Jun, J.S. White, M.L. Brongersma, Nat. Mater. 9 (2010) 193–204.
[29] H. Dai, M. Li, Y. Li, H. Yu, F. Bai, X. Ren, Opt. Express 20 (2012) 502–509.
[30] H. Dong, Z. Wu, F. Lu, Y. Gao, A. El-Shafei, B. Jiao, S. Ning, X. Hou, Nano Energ. 10 (2014) 181–191.
[31] E. Mulazimoglu, G. Nogay, R. Turan, H.E. Unalan, Appl. Phys. Lett. 103 (2013) 143124.
[32] Y. Wang, Y. Liu, H. Liang, Z. Mei, X. Du, Phys. Chem. Chem. Phys. 15 (2013) 2345–2350.
[33] B.T. Draine, P.J. Flatau, User guide for the discrete dipole approximation code DDSCAT 7.3. arXiv:1305.6497 [physics. comp-ph], 2013, http://arxiv.org/abs/1305.6497.
[34] P. Flatau, B. Draine, Opt. Express 20 (2012) 1247–1252.
[35] B.T. Draine, P.J. Flatau, J. Opt. Soc. Am. A 11 (1994) 1491–1499.
[36] D.M. O'Carroll, C.E. Hofmann, H.A. Atwater, Adv. M (2010) 1223–1227.
[37] O. Gunawan, S. Guha, Sol. Energ. Mat. Sol. C. 9 1388–1393.

[38] D. Kumar, S.K. Srivastava, P. Singh, M. Husain, V. Kumar, Sol. Energ. Mat. Sol. C. 95 (2011) 215–218.
[39] K.W. Kolasinski, Curr. Opin. Solid St. M. 9 (2005) 73–83.
[40] D.W. Lynch, W. Hunter, in: E.D. Palik (Ed.), Handbook of Optical Constants of Solids, Vol. 1, Academic Press, 1985, pp. 350–357.
[41] J. Geist, in: E.D. Palik (Ed.), Handbook of Optical Constants of Solids, Vol. 3, Academic Press, 1998, pp. 519–529.
[42] C. Mätzler, Res. Rep No. 2002-08, Inst. Angew, Phys. Bern, Switzerland (2002).
[43] C.F. Bohren, D.R. Huffman, Absorption and Scattering of Light by Small Particles, John Wiley & Sons, New York, 2008.
[44] A.R. Madaria, M. Yao, C. Chi, N. Huang, C. Lin, R. Li, M.L. Povinelli, P.D. Dapkus, C. Zhou, Nano Lett. 12 (2012) 2839–2845.
[45] P. Spinelli, M. Hebbink, R. De Waele, L. Black, F. Lenzmann, A. Polman, Nano Lett. 11 (2011) 1760–1765.
[46] H.A. Atwater, A. Polman, Nat. Mater. 9 (2010) 205–213.
[47] K. Catchpole, A. Polman, Opt. Express 16 (2008) 21793–21800.
[48] T.R. Jensen, G.C. Schatz, R.P. Van Duyne, J. Phys. Chem. B 103 (1999) 2394–2401.
[49] J. Peet, J. Kim, N.E. Coates, W.L. Ma, D. Moses, A.J. Heeger, G.C. Bazan, Nat. Mater. 6 (2007) 497–500.
[50] H.-P. Wang, T.-Y. Lin, C.-W. Hsu, M.-L. Tsai, C.-H. Huang, W.-R. Wei, M.-Y. Huang, Y.-J. Chien, P.-C. Yang, C.-W. Liu, ACS Nano 7 (2013) 9325–9335.
[51] S. Perraud, S. Poncet, S. Noël, M. Levis, P. Faucherand, E. Rouvière, P. Thony, C. Jaussaud, R. Delsol, Sol. Energ. Mat. Sol. C. 93 (2009) 1568–1571.
[52] A.E. Krasnok, A.E. Miroshnichenko, P.A. Belov, Y.S. Kivshar, JETP Lett. 94 (2011) 593–598.
[53] A.J. Haes, R.P. Van Duyne, J. Am. Chem. Soc. 124 (2002) 10596–10604.
[54] E. Ozbay, Science 311 (2006) 189–193.
[55] Y.H. Fu, A.I. Kuznetsov, A.E. Miroshnichenko, Y.F. Yu, B. Luk'yanchuk, Nat. Commun. 4 (2013) 1527.

Dr. Yingfeng Li is a lecturer of new energy materials at North China Electric Power University. He received his PhD degree in chemical engineering and technology from Tsinghua University in 2011. Currently, his primary research interests are in the optical properties of metal and semiconductor nanostructures, with significant current efforts devoted to understanding the light-harvesting behaviors of silicon nanowire.

Prof. Meicheng Li is the director of the Center for New Energy Materials and Photoelectric Technology at School of Renewable Energy in North China Electric Power University. His current focus is silicon nanowire based photovoltaic devices, including fundamental understanding, applied research and development (R&D), and flexible device design. He also has interest in R&D of perovskite solar cells, lithium ion battery system and other renewable energy (dye-sensitized solar cell, etc.).